A SELF-ASSEMBLY MECHANISM OF CUPROUS OXIDE NANOPARTICLES IN AQUEOUS COLLOIDAL SOLUTIONS

Yakui Bai, Tengfei Yang, Guoan Cheng, Ruiting Zheng

College of Nuclear Science and Technology, Beijing Normal University, Beijing, 100875 China

1 INTRODUCTION

The cuprous oxide and cupric oxide has been investigated for decades due to its unique semiconductor and optical properties. [1] As a P-type semiconductor material, the theoretical direct band gap of cuprous oxide is about 2.2eV. [2] Cuprous oxide has a very long excited lifetime (about 10μs), which can be used for photoluminescence. [3] Cuprous oxide has potential applications in solar cells, [4] nano-magnetic devices, [5] chemical industry, [6] sensors [7] and so on. It is also reported that cuprous oxide microspheres has been used as cathode material of lithium battery and photocatalyst in the visible light which led to photochemical decomposition of H_2O and generation of O_2 and H_2.[8] Structure-function relationship is the underlying motive for controlled fabrication of metal or semiconduct nanomaterial. [9]

In the past few years, numerous Cu_2O nanostructures, including nanoplates, [10] nanocubes, [11] octahedra, [12] spherical particles, [13] nanoboxes, [14] and nanowires [15] have been synthesized. The shape control and detailed crystal structure analysis of cuprous oxides have been performed on these Cu_2O nanocrystals. However, the growth mechanism, which is important for the controlled synthesis of Cu_2O nanocrystals, still needs a detailed investigation.

In this paper, we adopt an aqueous colloidal solution approach for the syntheses of monodispersed Cu_2O nanocubes, truncated nanocubes, cuboctahedra, nanosphere, and octahedra by adjusting experimental conditions, detect the influence of experimental conditions on the morphology evolution of Cu_2O nanocrystals. Based on our observation and analysis, the growth mechanism of Cu_2O nanocrystals is elucidated.

2 EXPERIMENTAL

Cu_2O nanoparticles were prepared by the reaction of cupric acetate with ascorbic acid at different temperatures. Typically, 0.25 mmol (0.05 g) of cupric acetate and 0.45 mmol (in repeating unit) of polyvinylpyrrolidone (PVP) were dissolved in 100 ml deionized water, 0.75 mmol (0.132 g) of ascorbic acid was dissolved in 15 ml of deionized water and 0.005 mol (0.2 g) of sodium hydroxide was dissolved in 20 ml of deionized water to form homogeneous aqueous solutions. Then the as-prepared sodium hydroxide solution (0.25

mol/L) was added dropwise into the cupric acetate solution (2.5 mmol/L) at room temperature, under vigorous stirring. The solution turned to be a blue suspension. Then the ascorbic acid aqueous solution (0.05 mol/L) was added into the above blue suspension at the speed of 3 drops per second under vigorous stirring. The color of the suspension changes from blue to green, finally, a reddish suspension was obtained after 10 minutes of reaction. The as-prepared products were centrifuged from the solution at 4000 rpm for 15 min by a Biofuges stratos centrifuger (Fisher Scientific). The derived products were washed with DI water three times and dried in air for characterization. By changing the molar ratio of copper acetate to cupric acetate, the amount of surfactant, the reaction temperature and the stirring rate, Cu_2O nanoparticles with different amorphous were obtained.

Crystal structure of the Cu_2O nanoparticle was identified by a powder X-ray diffractometer (XRD) (PANalytical X' Pert), employing Cu-Kα radiation (λ=1.5418Å) at 50 kV and 200 mA. The size and morphology of the Cu_2O nanoparticles was observed by a field emission scanning electron microscopy (SEM) (Hitachi S-4800, Japan) at 5 kV. Crystal structure and growth orientation of the Cu_2O nanoparticles was characterized by a high resolution transmission electron microscopy HRTEM (Philips FEI TECNAI F30) at 200 kV. The ultraviolet and visible light (UV-vis) absorption spectra was recorded by a Shimadzu UV-365 PC spectrophotometer.

3 RESULTS AND DISCUSSIONS

Figure 1 illustrates the microstructures of typical Cu_2O nanocubes synthesized using our approach. Figure 1 A shows a SEM image of the samples. The nanoparticles exhibit typical cubic morphology with a mean edge length of 255 nm and a standard deviation of 35 nm. It could be observed that the corners of some nanocubes were truncated. Figure 1B shows the TEM image of a Cu_2O nanocube on the surface of a TEM grid. The inset shows the selected area electron diffraction (SAED) patterns obtained by directing the electron beam perpendicular to the square faces of the cube, The square symmetry of this pattern indicates that each Cu_2O nanocube was a single crystal bounded mainly by {100} facets. Figure 1 C is the XRD pattern of a reaction product in the 2θ range of 10-80 °. The pattern could be distinctly indexed to a cubic phase with lattice constants a=4.267Å for Cu_2O ((JCPDS No. 78-2076). It is worth noting that the ratio between the intensities of the (200)

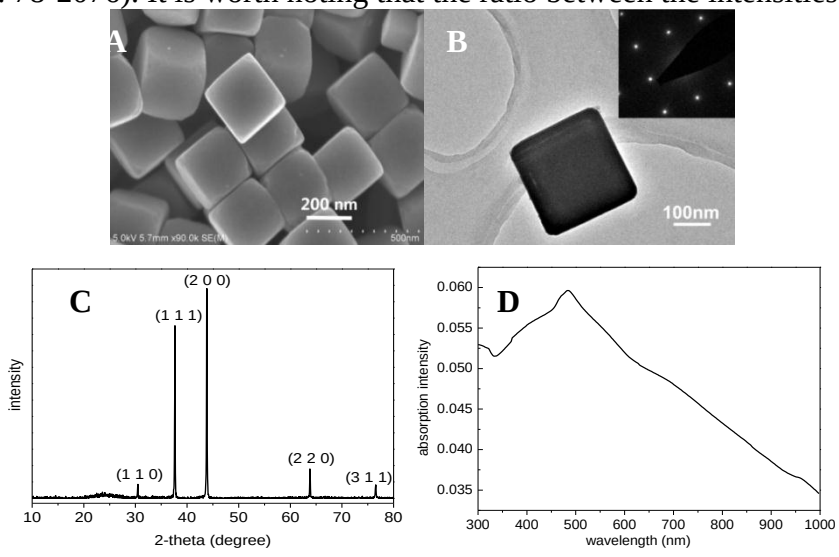

Figure 1 *(A) SEM images of Cu_2O nanocubes synthesized via a typical procedure described in the experimental section. (B) TEM images of Cu_2O nanocubes synthesized in a typical procedure. (C) XRD pattern of as-prepared samples obtained by the typical synthetic process. (D) UV-visible spectrum recorded from solution of cuprous oxide nanocubes dispersed in deionized water at room temperature.*

and (111) diffraction peaks was higher than the conventional value (1.28 versus 0.435), indicating that our nanocubes were abundant in {100} facets. Truncated corner of Cu_2O nanocubes correspond to {111} facets. UV-vis absorption spectra of cuprous oxide nanoparticles was demonstrated in Figure 1 D. The characteristic absorption peak is due to plasma resonance excitation of copper atoms on the surface of nanocubes.[16] The absorption peak lies around 484 nm. The calculated direct band gap of our cuprous oxide is 2.56 eV, slightly larger than the theoretical direct band gap of 2.2 eV.

The morphology and the size of the nanoparticles could be tuned by adjusting the reaction conditions such as reaction temperature, reactant concentration, amount of surfactant, and stirring rates. In order to elucidate the effect of experimental parameter on the morphology of Cu_2O nanocrystals, we carry out four sets of experiments. In each set of experiments, we only change one parameter and other parameters are kept the same as that of typical synthesis parameters in experimental section.

Figure 2 shows the Cu_2O nanoparticles synthesized in our experiments. Figure 2 A1-A4 reveal the morphologies of Cu_2O nanoparticles synthesized at different amount of surfactant. Without surfactant, only irregular nanoparticles are observed. By the help of surfactant, regular truncated nanocubes form. When the amount of surfactant increased from 0.18 mmol to 0.45 mmol, the average particle size changed from 100 nm to 500 nm. The presence of PVP seems beneficial to the growth of Cu_2O nanocubes.

Temperature is a key factor in preparing uniform cubic Cu_2O particles. Figure 2 B1-B4 show the SEM images of Cu_2O nanocubes prepared at 30 ℃, 40 ℃, 50 ℃ and 90 ℃, respectively. The morphology of particle changes from truncated cube to perfect cube with temperature arising from 30 ℃ to 50 ℃, particles in three samples have smooth surface and good uniformity. Nanocubes prepared at 90 ℃ are corroded seriously and display uneven surfaces. With the rising of synthesis temperature, the average edge length of nanocubes exhibits a peak (500 nm) at 50 ℃.

The reactant concentration is another key factor that influences the morphology of Cu_2O nano particles. According to our observation, at different copper acetate concentration, the most particles are truncated cube, except that the particle size varies form 100 nm to 1700 nm with the increase of copper acetate concentration. However, the amount of reducing agent will result in different morphology of productions. Figure 2 C1-C4 are SEM images of Cu_2O nanocubes prepared by 0.25, 0.5, 0.75 and 1 mmol of ascorbic acid respectively. When the amount of reducing agent was less than 0.25 mmol, the product mainly comprise of $Cu(OH)_2$ nanowire. When the amount of reducing agent reaches 0.75 mmol, truncated cuprous oxide nanocubes with the average

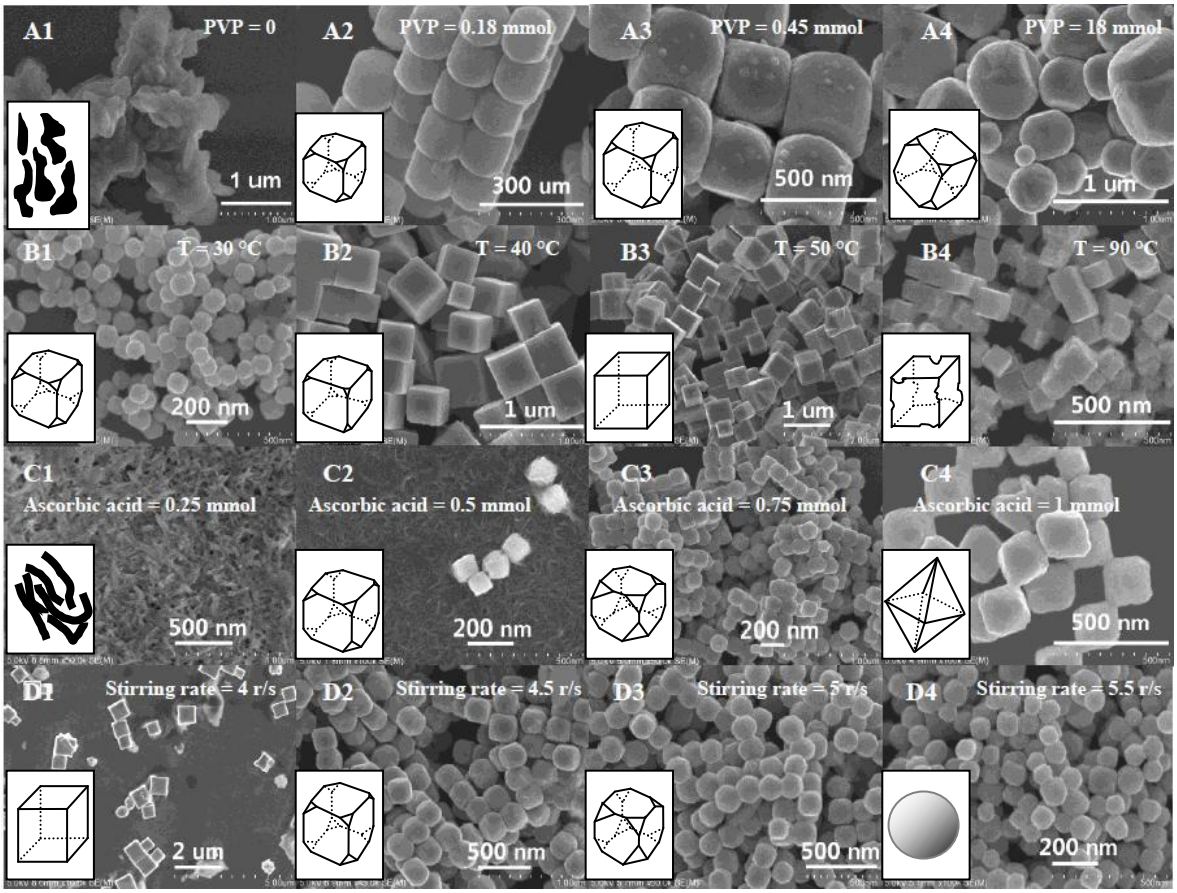

Figure 2 *SEM images of Cu_2O nanoparticles fabricated by different reaction conditions. Images in row A to D are the changes of reaction conditions including amount of surfactant, temperature, amount of reducing agent and stirring rate respectively. A1 to A4 are the amount of PVP changing from 0 to 0.018 mol. B1 to B4 are the temperature varied from 30 ℃ to 90 ℃. C1 to C4 are the amount of ascorbic acid was increased from 0.000246 mol to 0.000984 mol. D1 to D4 are stirring rate was increased from 4 r/s to 5.5 r/s.*

diameter about 200 nm are obtained. The shape of cuprous oxide particle turns to rough octahedron with the amount of reducing increasing to 1 mmol. When the amount of reducing agent was further increased to 1.25 mmol, there is no precipitation in solution after reaction.

An interesting finding in our experiment is that the morphology of nanoparticles was very sensitive to the stirring rate. Small adjusting of stirring rate will result in great changes of particle morphology. Figure 2 D1-D4 indicated the SEM image of Cu_2O nanoparticles synthesized at 4 r/s, 4.5 r/s, 5 r/s, 5.5 r/s of stirring rate respectively. The shape of nanoparticles changes from cube to truncated cube and then to spheres. At the same time, the average particle size decreases from 750 nm to 150 nm with the increase of stirring rate.

4 DISCUSSION

We speculate that Cu_2O tends to form nanocubes due to orientational crystallization mechanism. Cupric acetate could be dissolved in water and forms a uniform ionic solution. When the NaOH is added in the solution, the Cu^{2+} react with OH^- and forms blue insoluble

$Cu(OH)_2$ precipitate. While $Cu(OH)_2$ suspension react with ascorbic acid, $Cu(OH)_2$ will be reduced into reddish Cu_2O nanoparticles. The reactions can be expressed as:

$$Cu^{2+} + 2OH^{-} \rightarrow Cu(OH)_2 \downarrow \quad (1)$$

$$Cu(OH)_2 + C_6H_8O_6 \rightarrow Cu^{2+} + 2H_2O + C_6H_6O_6^{2-} \quad (2)$$

$$2Cu^{2+} + C_6H_6O_6^{2-} + H_2O \rightarrow Cu_2O + C_6H_6O_6 + 2H^{+} \quad (3)$$

When the Cu_2O precipitate from the solutions, they tend to aggregate and to reduce their total surface energy. When subsequent Cu_2O monomers precipitate from the solution, they tend to aggregate on the existing Cu_2O seeds and grow up. In the absence of a hard template, low-dimensional structures are governed by thermodynamic (e.g., temperature, reduction potential) and kinetic (e.g., reactant concentration, diffusion, solubility, reaction rate) parameters.

It is reported that PVP has the selective adsorption properties to specific crystal planes, and could be used to kinetically control the growth of single-crystalline nanocubes. We also find that surfactant plays an important role on morphology and size of nanocrystals. Without PVP surfactant, the structure of products is polycrystalline cluster without certain morphology, which indicates Cu_2O nanoparticles aggregate in a disorder manner. When PVP was added into solution, monodispersed colloidal solutions of Cu_2O nanocrystals with regular polyhedral shapes and bound entirely by {100} and {111} facets of the fcc crystal lattice are obtained. It is observed that the Cu_2O nanocubes with larger particle size are obtained at high PVP concentration which indicates that the existence of PVP promote the growth of Cu_2O nanocubes. We conjecture that the interaction between PVP and Cu_2O monomer raises the critical nucleation energy, which suppresses the nucleation rate and makes Cu_2O nanocubes grow faster.

As an important thermodynamic parameter, temperature exhibits a significant influence on the morphology of nanocrystals. At the room temperature, by the help of surfactants (it is believed that the selective interaction between PVP and {100} planes of Cu_2O could greatly reduce the growth rate along the <100> direction), [17] truncated Cu_2O nanocubes are synthesized. From energy point of view, this structure is stable. Because the corners of nanocube have larger specific surface area, the corners of nanocubes are corroded and truncated along the {111} planes. With the rising of synthesis temperature, diffusion and migration rate of the ions and monomers increase, the nanocubes grow fast along the <111> directions. Morphology of product changed gradually from truncated nanocube to nanocube. At the same time, particle size increased significantly. However, too high temperature will result in heavy corrosion of cube surface.

Ascorbic acid is a mild reducing agent, it could reduce $Cu(OH)_2$ and forms Cu_2O nanocubes. At the same time, Ascorbic acid works as a vinylogous carboxylic acid. Excessive ascorbic acid will corrode the Cu_2O nanocubes via a dismutation reaction. Since the {100} planes of nanocubes are selective adsorbed by capping agent PVP, {111} planes become candidates for selective corrosion. With the increase of the amount of ascorbic acid, the morphology of Cu_2O nanocubes varies from truncated cube to cuboctahedra and further becomes octahedron. Further increase the amount of ascorbic acid will cause the completely corrosion of Cu_2O nanoparticles, and the suspension turns to be transparent solution again. This finding is of great value, because previous report indicates that {111} planes of Cu_2O particles have high catalytic activity.[18,19] In addition to the thermodynamic and kinetic parameters, the shape of Cu_2O nanocrystal is sensitive to the stirring rate. In fact, the rapid stirring rate actually hinders the combination between different particles and prevented the crystal from growth.

Moreover, the high stirring rate will enhance the probability and energy of collision between particles and wall (or between themselves). Mechanical wear and erosion make the corners and edges of Cu_2O nanocubes disappear gradually. When the stirring rate is 4 r/s, perfect cuprous oxide nanocubes with average edge length of 750 nm are synthesized. While the stirring rate increase to 5 r/s, truncated cubes with the average diameter of 250 nm are formed in solution. When stirring rate reaches 6 r/s, only 150 nm diameter of nanospheres can be found in the product.

5 CONCLUSION

In this paper, cuprous oxide nanoparticles with different morphologies have been successfully synthesized by a wet-chemical approach in aqueous solution. XRD and TEM results indicate that the cuprous oxide particles are truncated nanocubes bounded by {100} and {111} facets. By the adjusting of synthesis conditions, Cu_2O nanocubes, truncated nanocubes, cuboctahedra, nanosphere, and octahedra are synthesized. Growth mechanism of these nanoparticles is interpreted as the combination effects of selective growth, selective corrosion and mechanical erosion of Cu_2O nanocrystals. These Cu_2O nanoparticles should find applications in a variety of areas such as photonics, catalysis, and sensing. This work indicate that Cu_2O nanoparticles with well-controlled shapes, sizes, and structures can be obtained by the optimization of thermodynamic and kinetic parameters.

References

1 I. Grozdanov, *Mater. Lett.*, 1994, **19**, 281.
2 P.B. Ahirraoa, B.R. Sankapalb and R.S. Patil, *J. Alloy. Compd.*, 2011, **59**, 5551.
3 R.M. Habiger and A. Compaan, *Solid State Commun.*, 1976, **18**, 1531.
4 L. F. Gou and C. J. Murphy, *Nano Lett.*, 2003, **3**, 231.
5 Asar Ahmed, Namdeo S. Gajbhiye and S. Kurian, *J. Solid State Chem.*, 2010, **183**, 2248.
6 W. Z. Wang and W. J. Zhu, *J. Phys. Chem. B*, 2006, **110**, 13829.
7 Jun Liu, Shaozhen Wang, Qian Wang and Baoyou Geng, *Sensor Actuat. B*, 2009, **143**, 253.
8 M. Hara, T. Kondo, M. Komoda, S. Ikeda, K. Shinohara, A. Tanaka, J. N. Kondo and K. Domen, *Chem. Commun.*, 1998, **3**, 357.
9 Yugang Sun and Younan Xia, *Science*, 2002, **298**, 2176.
10 Chun-Hong Kuo and Michael H. Huang, *Nano Today*, 2010, **5**, 106.
11 Zhenghua Wang, Hui Wang, Lingling Wang and Ling Pan, *J. Phys. Chem. Sol.*, 2009, **70**, 719.
12 Xu Zhang, Yi Xie, Fen Xu, Xiaohui Liu and Di Xu, *Inorg. Chem. Commun.*, 2003, **6**, 1390.
13 Haolan Xu, Wenzhong Wang and Wei Zhu, *Micropor. Mesopor. Mat.*, 2006, **95**, 321.
14 Lei Huang, Feng Peng, Hao Yu and Hongjuan Wang, *Mater. Res. Bull.*, 2008, **43**, 3407.
15 Ho Sun Shin, Jae Yong Song and Jin Yu, *Mater. Lett.*, 2009, **63**, 397.
16 M. Y. Shen, T. Yokouchi, S. Koyama, and T. Goto, *Phys. Rev. B*, 1997, **56**, 13066.
17 E. Ko, J. Choi, K. Okamoto, Y. Tak and J. Lee, *ChemPhys.* Chem., 2006, **7**, 1505.
18 P. He, X. Shen and H. J. Gao, *Colloid Interface Sci*., 2005, **284**, 510.
19 H. Xu, W. Wang and W. Zhu, *J. Phys. Chem.B*, 2006, **110**, 13829.